The EMBO Journal vol.15 no.24 pp.6841–6846, 1996

Adenovirus 3 penton dodecahedron exhibits structural changes of the base on fibre binding

Guy Schoehn, Pascal Fender, Jadwiga Chroboczek and Elizabeth A.Hewat[1]

Institut de Biologie Structurale Jean-Pierre Ebel, 41 av. des Martyrs, 38027 Grenoble, France

[1]Corresponding author

It was recently shown that co-expression of adenovirus type 3 (Ad3) penton base and fibre in the baculovirus system produces dodecahedral particles, as does the expression of the penton base alone. The structure of both of these dodecahedral particles, with and without fibre, has been determined by cryoelectron microscopy and 3-dimensional reconstruction techniques to a resolution of 25 and 20 Å, respectively. The general form of the penton base resembles that of the base protein in the recent reconstruction of adenovirus type 2. There is a remarkable difference in the penton base structure with and without the fibre. The five small protuberances on the outer surface of each base move away from the 5-fold axis by ~15 Å when the fibre is present. These protuberances are of relatively low density and most probably represent a flexible loop possibly containing the RGD site involved in integrin binding. The fibre is apparently bound to the outer surface of the penton base, rather than inserted into it. The fibre is flexible and the shaft contains two distinct globular regions 26 Å in diameter. The volume of the inner cavity of the dodecahedron is 350 ± 100 nm^3. This small volume precludes the use of the inner cavity to house genetic information for gene therapy; however, the possibility remains of linking the gene to the dodecahedron surface in the hope that it will be internalized with the dodecahedron.

Keywords: adenovirus 3/cryo-electron microscopy/dodecahedron/gene therapy/3-D reconstruction

Introduction

Small dodecahedral particles were seen in adenovirus type 3 (Ad3) preparations by electron microscopy as early as 1964 (Norrby, 1964). These dodecahedron particles are apparently an association of 12 Ad3 pentons. Recently, the two penton proteins base and fibre of adenovirus 3 were co-expressed in a baculovirus system and dodecahedral particles formed spontaneously (Fender *et al.*, 1997). This observation has opened up interesting possibilities not only for gene therapy (Fender *et al.*, 1997), but also for the study of the penton base–fibre interaction. Infection by adenoviruses is unusual in that two cell recognition sites appear to be involved (Philipson *et al.*, 1968; Wickham *et al.*, 1993; Cuzange *et al.*, 1994; Henry *et al.*, 1994; Louis *et al.*, 1994). The first, on the knob of the fibre, recognizes a cell receptor. The second, probably involving an RGD sequence on the base, takes part both in the attachment to an integrin and in the virus internalization. The expressed dodecahedra are made of the viral proteins responsible for the attachment and internalization properties of the adenovirus.

Adenoviruses are non-enveloped double-stranded DNA viruses which are responsible for conjunctivitis, rhinopharyngitis and enteric disease in humans (Horwitz, 1990). They are of considerable use as model systems in molecular biology and have been extensively studied. The ability of the adenovirus to infect a wide range of cell types and their relatively large DNA capacity have made them of great interest as viral vectors in gene therapy (Fitzgerald *et al.*, 1983; Yoshimura *et al.*, 1993; Yang *et al.*, 1995). The adenovirus capsid is ~900 Å in diameter with a fibre protein protruding outwards from each of the 12 icosahedral vertices. The virion contains at least 11 proteins (polypeptides II–IX, IVa, μ, terminal) whose position and role are becoming clearer (Stewart *et al.*, 1991, 1993). The major capsid proteins are 240 hexons and 12 pentons at each of the 5-fold vertices. The pentons consist of a pentameric base to which a trimeric fibre protein is attached non-covalently. The fibre contains three regions: the N-terminal tail which is attached to the base, a shaft of serotype-dependent length and a globular C-terminal knob. The amino acid sequence of the shaft contains a repeat motif of ~15 residues (Green *et al.*, 1983; Stouten *et al.*, 1992). The length of the shaft ranges from six repeating motifs in Ad3 to 22 in Ad2 and Ad5, i.e. from 120 to 330 Å in length (Signäs *et al.*, 1985; Devaux *et al.*, 1987; Ruigrok *et al.*, 1990; Chroboczek *et al.*, 1995). The X-ray structures of the hexon of Ad2 (Roberts *et al.*, 1986) and the knob of Ad5 fibre protein are known (Xia *et al.*, 1994).

Stewart *et al.* determined the structure of the native Ad2 virion to 35 Å resolution (Stewart *et al.*, 1991) and then to 25 Å resolution (Stewart *et al.*, 1993) using cryo-electron microscopy and three-dimensional (3-D) reconstruction. They visualized the overall architecture of the virion, including the penton base and roughly the first 88 Å of the fibre at the same density level. The 330 Å long fibre of Ad2 is evidently very flexible and hence cannot all be seen in the reconstruction. By combining the cryo-electron microscope data with the X-ray structural data on the hexon to generate difference maps, Stewart *et al.* determined the form and location of six different proteins in the Ad2 capsid. In particular, they located four proteins involved in cementing and stabilizing the rather complex Ad2 capsid.

In this paper, we present the cryo-electron microscopy and 3-D reconstructions of the dodecahedron of the expressed Ad3 penton both with and without the fibre.

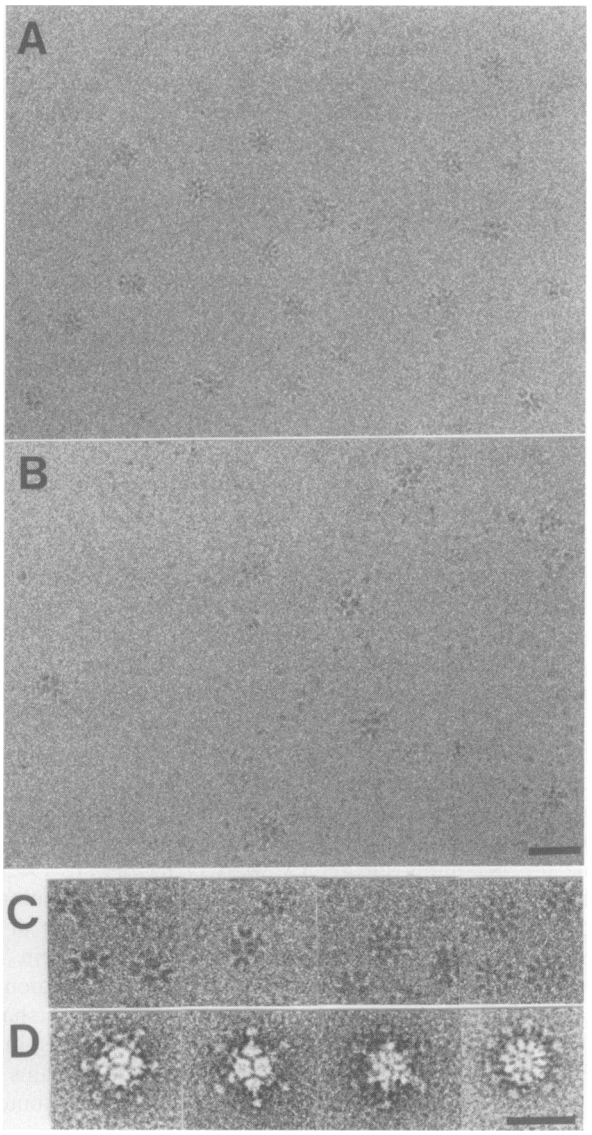

Fig. 1. Electron micrographs of frozen–hydrated Ad3 dodecahedra without (**A**) and with (**B**) fibre. They are the more highly defocused image pair used in the preliminary low-resolution reconstruction. The defocus is ~3.5 μm. (**C**) and (**D**) Enlargements of Ad3 dodecahedra seen down the 2-, 2-, 3- and 5-fold axis (from left to right). (C) Frozen–hydrated without fibre. (D) Negatively stained in uranyl acetate with fibre. Scale bars = 500 Å

The small diameter of the Ad3 dodecahedron, compared with the native virion, makes the Ad3 dodecahedron a more difficult object for structural studies than the large native virion, but the shortness of the Ad3 fibre allows visualization of its entire length. The aims of this study were to determine the size of the inner cavity of the dodecahedron because of its potential use as a gene carrier, to visualize the attachment of the fibre to the base and to determine whether structural changes occur on binding of the fibre to the base.

Results and discussion

Cryo-electron microscopy of Ad3 dodecahedra

The electron microscope images of frozen–hydrated Ad3 dodecahedra reveal well-formed particles with a highly textured surface (Figure 1). The knob, and in some cases the fibre, is visible in high-defocus images and the orientations of some of the particles in high-symmetry orientations can be seen directly. The use of spun columns to remove isolated monomers was more effective in the case of dodecahedra without fibre than with fibre. Even after two passages through spun columns, monomers are visible in the background of the preparation with fibre. It appears that the equilibrium dodecahedra–penton is reached very rapidly and that the dodecahedra without fibre is more stable under the conditions used here.

Reconstructed density of the Ad3 dodecahedra

The isosurface representations of the reconstructed Ad3 dodecahedron with and without fibre (Figure 2A and B) reveal essentially the same external features as for the penton base of Ad2 (Stewart *et al.*, 1991, 1993). We have used this similarity to choose the hand of our reconstructions. Stewart *et al.* (1991) were able to determine the absolute hand of their reconstruction using additional information on the X-ray structure of the hexon and electron microscope data on a capsid dissociation fragment of Ad2, called the group of nine hexons (Laver *et al.*, 1969; Nermut, 1984; Furcinetti *et al.*, 1989). The diameter of the base at its widest point is 95 Å in both the dodecahedron with and without fibre, cf. 112 Å for the Ad2 base. The base height, including the five low-density protuberances, is roughly 124 Å, cf. 124 Å for Ad2. The penton base appears hollow inside, but there is no evidence of a 30 Å hole in the base into which the fibre is inserted, as was previously assumed (van Oostrum *et al.*, 1987; Ruigrok *et al.*, 1990; Stewart *et al.*, 1991). However, there is probably a communicating hole between the hollow interior of the base and the inner cavity of the dodecahedron. The internal cavity of the dodecaheron is ~8.7 nm in diameter so the volume is 350 ± 100 nm^3. In the dodecahedron, each penton base is bound to five neighbouring pentons, whereas in the adenovirus each penton is bound to five peripentonal hexons. The region of the penton involved in penton–penton and penton–hexon binding is roughly the same [Figure 3E and F, and Stewart *et al.* (1993) Figure 3C].

As for the Ad2 penton, there are five small protuberances on each penton base. The density in these protuberances is only 50% of the maximum density in the rest of the base (Figure 3). The contour threshold in Figure 3C has been chosen so that the total enclosed volume estimated for the dodecahedron equals the estimated volume, assuming a protein density of 1.3 g/cm^3 and a mol. wt of 430 kDa per penton. In all other isodensity figures, a slightly lower threshold has been used to show the low-density protuberances. An explanation for the low density is that the protuberances represent flexible loops. It will be recalled that the highly immunogenic loop of viral protein 1 of foot-and-mouth disease virus (FMDV) is a highly flexible loop which contains the RGD integrin receptor site and is seen by X-rays as a zone of low density. The structure of the FMDV serotype C 15 residue immunogenic loop complexed with a neutralizing Fab is known (Verdaguer *et al.*, 1995) and may be fitted (with room to spare) into the low-density protuberances of the Ad3 penton base (Figure 4). Mathias *et al.* (1994) used structure prediction algorithms which predicted that the conserved RGD sequence lies at the apex of two extended α helices.

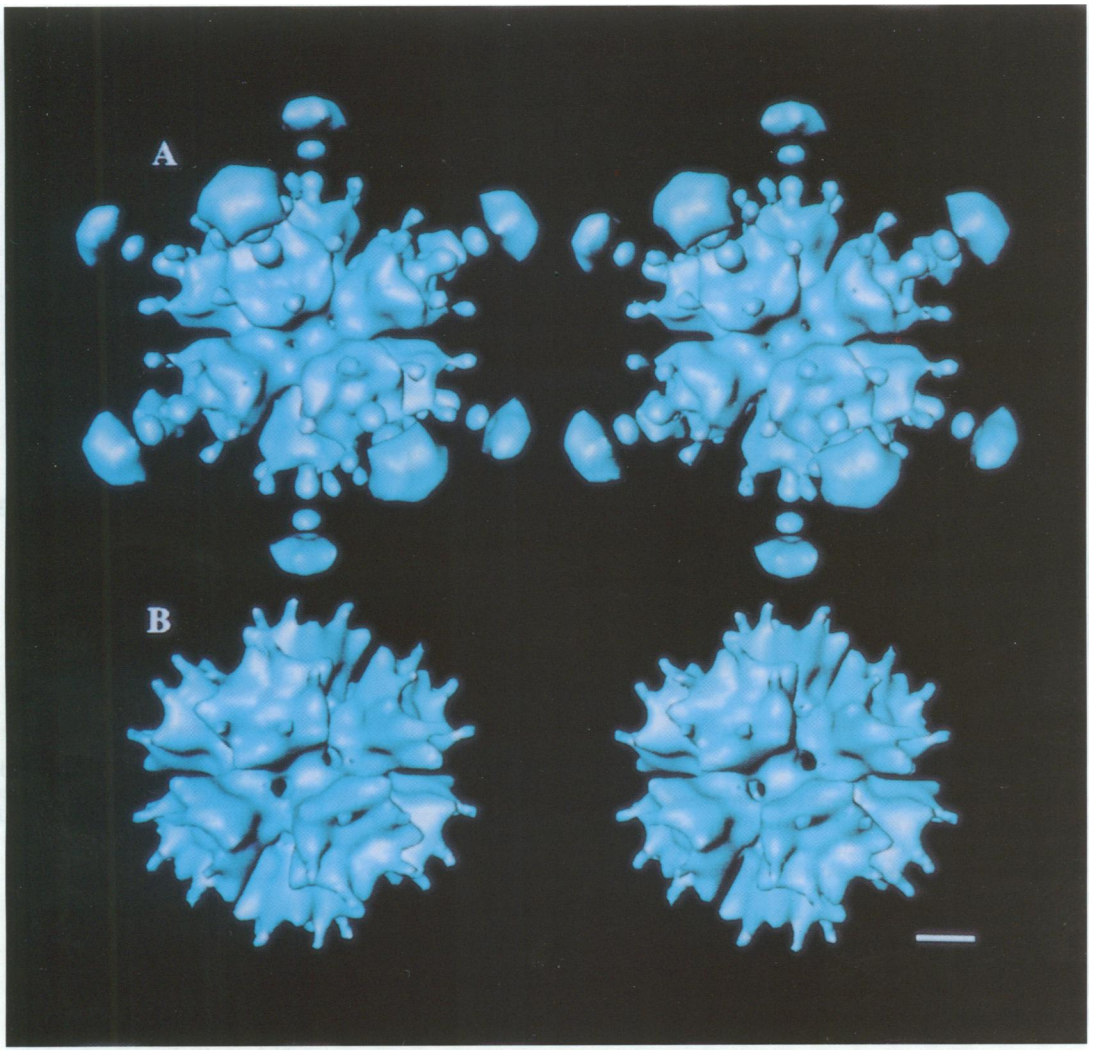

Fig. 2. Stereo views of the isosurface representations of the Ad3 dodecahedron with fibre, viewed down a 2-fold axis (**A**) and without fibre (**B**). Only the front half of the dodecahedra are represented. Scale bar = 50 Å.

This and the hydrophobic nature of the residues flanking the RGD sequence argue in favour of an exposed loop structure. Thus, it is possible that the five protuberances on each penton base each represent a flexible loop containing the RGD site.

The X-ray structure of the Ad5 knob (Xia *et al.*, 1994) fits well in size the Ad3 reconstructed density (Figure 4). The density of the knob has been 5-fold averaged so no detailed fit is possible. Also, the question of how the trimeric fibre binds to the pentameric base remains open. In reconstructing the dodecahedra, icosahedral symmetry is necessarily imposed. There is no obvious way of reconstructing the fibre with the correct 3-fold symmetry.

The fibre–base interaction

The fibre has a total length of 13.6 nm (Figure 3), cf. 16.0 ± 1.4 nm measured in negative stain (Ruigrok *et al.*, 1990). The tail of the fibre is spread out over a large area of the base at least 4.0 nm in diameter. It interacts with the outer surface of the base rather than being inserted into a pre-existing hole. The fibre shaft has a distinctly beaded appearance, as has been previously observed in shadowed images of Ad2 fibre (Ruigrok *et al.*, 1990) and in the first 88 Å of the reconstructed Ad2 fibre (Stewart *et al.*, 1991). In fact, there is good agreement between the first 88 Å of the reconstructed Ad2 fibre (Stewart *et al.*, 1991) and the total length of the Ad3 fibre shaft (without the knob) which consists of two globular regions roughly 26 Å in diameter and separated by 35 Å. A beading pattern with a spacing of 35 Å was also observed in negatively stained isolated fibres of Ad2 (Ruigrok *et al.*, 1990). The relationship between this beaded fibre structure and the six hydrophobic repeating motifs in the fibre sequence (Kidd *et al.*, 1993) is not evident. There are apparently three motifs per globular (bead) domain.

The reconstructed map for the dodecahedron without fibre showed no change after about three cycles of refinement. On the contrary, the reconstructed map for the dodecahedron with fibre did not reach a completely stable result, particularly for the fibre density. The fibre density was more or less smeared out, as would be expected if the fibre was flexing from a point half way along its length. Stewart *et al.* (1991) observed a similar flexing of the Ad2 fibre, which smeared out all but the 88 Å of the fibre closest to the capsid. The final map was chosen on the basis of highest contrast in the fibre. The final

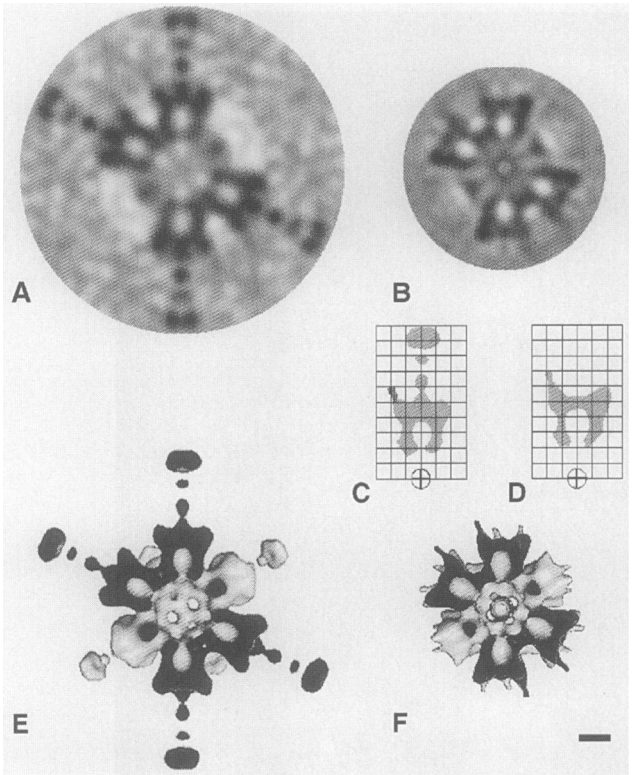

Fig. 3. Sections through the origin of the reconstructed density maps of the Ad3 dodecahedra with (**A**) and without (**B**) fibre, viewed down a 2-fold axis. A section through the penton which passes through the low-density protuberances on the dodecahedron with fibre (**C**) and without fibre (**D**). The hatched region in (C) represents the additional low-density protuberance visible when the threshold is lowered. The grid spacing is 25 Å. Isosurface representations of the Ad3 dodecahedron with fibre (**E**) and without fibre (**F**) viewed down a 2-fold axis. Only the back half of the dodecahedra are represented. The dark regions in (E) and (F) represent cut surfaces. Scale bar = 50 Å.

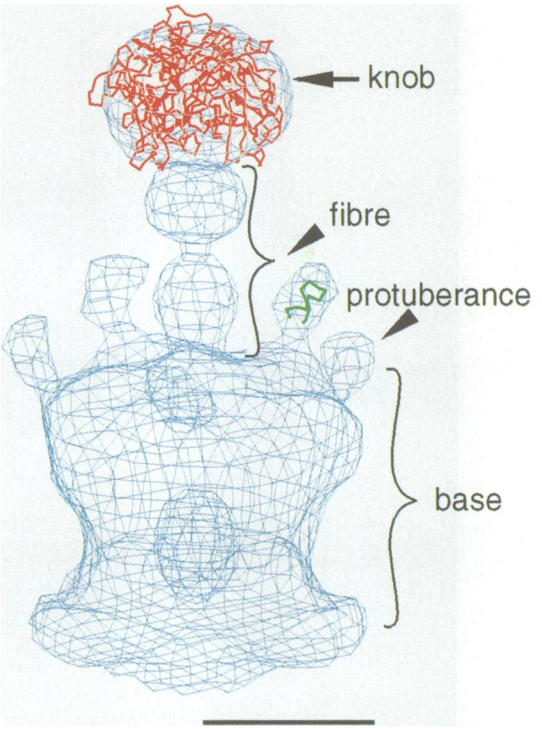

Fig. 4. Fit of the X-ray structures of the RGD-containing loop of FMDV (green) and the knob of Ad5 (red) to the cryo-electron microscope reconstructed density of Ad3 dodecahedron (blue). Scale bar = 50 Å.

reconstruction of the dodecahedron without fibre was made from 34 particles and included information to 20 Å resolution. The particle orientations were well dispersed over the asymmetric unit triangle (Figure 5). The phase residual went to 90° at roughly 20 $Å^{-1}$ and all the inverse eigenvalues were <0.1. The final reconstruction of the dodecahedron with fibre was made from 26 particles and included information to 25 Å resolution. The phase residual went to 90° at 24 $Å^{-1}$ and all the inverse eigenvalues were <0.1.

Effect of fibre binding on the structure of the penton base

Comparison of the reconstructions of the dodecahedron with and without fibre (Figure 6) reveals remarkable differences in the five protuberances on the penton base. They move away from the 5-fold axis by ~15 Å when the fibre is bound. If the assignment of these protuberances to a flexible loop containing the RGD integrin binding site is correct, it follows that the observed difference probably has a functional significance for the entry of the adenovirus into the cell.

Also, both density maps show the penton base to be hollow inside, but there is no hole in the base at the interface between the base and the fibre. The fibre is

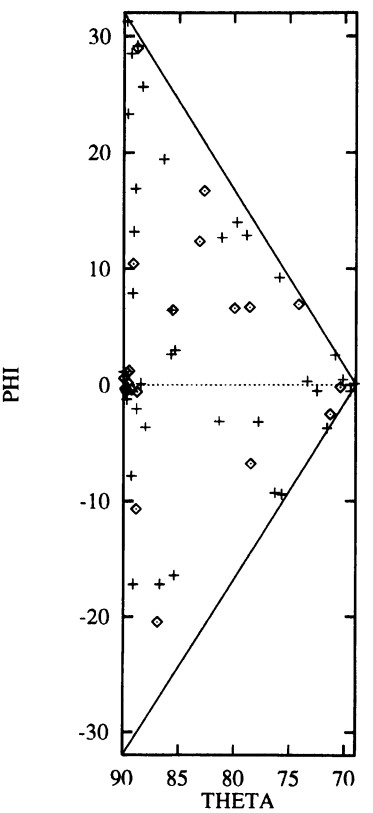

Fig. 5. Refined orientation parameters, θ and ϕ of the 26 Ad3 dodecahedron with fibre (diamonds) used in the reconstruction shown in Figure 2A and of the 34 Ad3 dodecahedron without fibre (+) used in the reconstruction shown in Figure 2B.

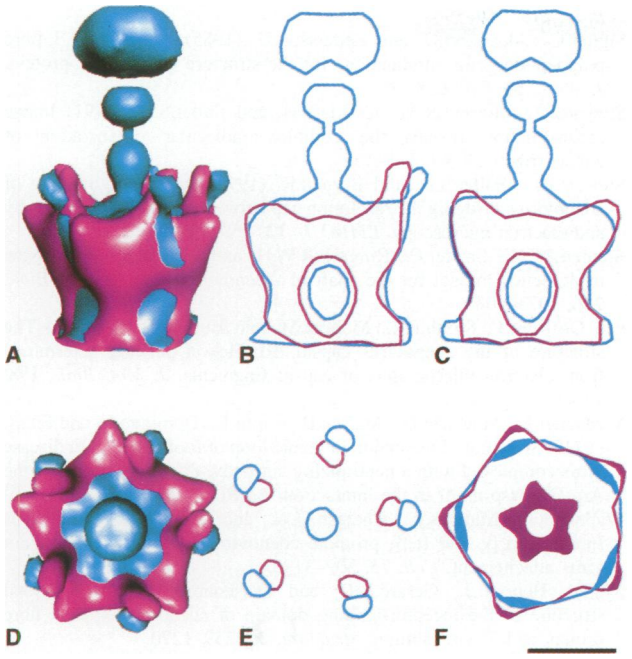

Fig. 6. Comparison of the reconstructed Ad3 penton with (blue) and without (magenta) fibre. For better comparison, both reconstructions are restricted to 25 Å resolution. Side view of one penton (**A**) and corresponding sections through the axis of the fibre showing the isodensity surfaces (**B** and **C**). Top view of one penton (**D**) and corresponding sections perpendicular to the axis of the fibre showing the isodensity surface through the low-density protrusions and through the widest section of the base (**E** and **F**). Scale bar = 50 Å.

apparently bound to the outer surface of the base. Given the change in position of the protuberances on binding of the fibre, there is clearly some rearrangement of the base. The difference in the maps at the inner cavity cannot be interpreted with certainty because the maps become less reliable towards the centre. Also, while a correction has been made to minimize the difference in contrast transfer function (CTF) of the images used in these two reconstructions, only reconstructions of both dodecahedra from the same image will completely eliminate all imaging-related differences. However, differences in the CTF will essentially cause differences in the size and not in the position of density regions. The CTF correction made to the reconstruction without fibre, for comparison with the reconstruction with fibre, did not change the position of the protuberance at all.

The inner cavity of the Ad3 dodecahedron

The volume of the inner cavity of the Ad3 dodecahedron at 350 ± 100 nm^3 is small compared with the Ad2 virion, which has a volume of ~165 000 nm^3 (Stewart *et al.*, 1991), and contains 36 000 bp. It follows that ~80 bp can fit into the Ad3 dodecahedron assuming the same DNA packing density. This precludes the use of the inner cavity of the dodecahedron to house genetic information for gene therapy; however, the possibility remains of linking the gene to the dodecahedron surface in the hope that it will be internalized with the dodecahedron.

Materials and methods

Growth and purification of adenovirus 3 dodecahedra

Dodecahedra were prepared after the method of Fender *et al.* (1997) using recombinant baculoviruses. Immediately prior to the preparation of frozen–hydrated specimens for electron microscopy, excess monomers were removed by passage through a Sepharose S300 spun column (Pharmacia).

Preparation and observation of electron microscope specimens

Negatively stained specimens of dodecahedron were prepared in uranyl acetate by standard techniques as described in Hewat *et al.* (1992a) and observed at 80 kV in a ZEISS 10C electron microscope.

Frozen–hydrated specimens were prepared on holey carbon films as described by Hewat *et al.* (1992a). A 4 µl sample of the specimen was applied to non-glow discharged holey carbon film on a 400 mesh copper grid, blotted with filter paper for 1–2 s and rapidly plunged into liquid ethane at –175°C. Specimens were observed at a temperature of close to –180°C using a Gatan 626 cryo-holder in a Phillips CM200 operating at 200 kV. Images were obtained under low-dose conditions (<10 e/Å^2) at a nominal magnification of ×27 500, and 1.2 and 3.5 µm underfocus. The images were recorded on KODAK SO163 electron image films and developed in full-strength D19 developer for 12 min at room temperature. The magnification was calibrated in an independent experiment using the 23 Å pitch of tobacco mosaic virus.

Image analysis

Preliminary selection of micrographs for analysis was performed as described previously (Hewat *et al.*, 1992b). Defocus pairs were digitized using an Optronics microdensitometer coupled to a PC, with a step size of 12.5 µm, which corresponds to a pixel size of 4.55 Å at the specimen, taking into account the corrected microscope magnification of ×28 500. Particle image selection and pre-processing were performed on a Silicon Graphics computer using the Semper 6 Plus image-analysis package. Images were re-interpolated to a pixel size of 1.5 times the original so that 128×128 files could be used. The selected particles were masked, normalized by subtracting the mean and any density gradient present, and normalizing the standard deviation. The particle images further from focus were pre-centred by cross-correlation with the radially averaged summation of several particle images. The particle images closer to focus had too little contrast for direct particle selection and centring. They were therefore selected and centred by cross-correlation with their high-defocus image pair.

Further image analysis was performed on a DEC Alpha using modified versions of the MRC icosahedral programs and model-based programs (Baker and Cheng, 1996) supplied by S.Fuller (Fuller *et al.*, 1996). The dodecahedron with fibre was the first to be analysed and the method of common lines (Crowther, 1971) was used for the determination of particle origins and orientations for the high-defocus image only. The model-based programs were used for all subsequent orientation and origin determinations. The reconstructed dodecahedron with fibre was used as a starting model for the analysis of the dodecahedron without fibre. In each case, the cycle of refinement consisted of: (i) determining the origins and orientations for the high-defocus image using the model-based approach; (ii) using the origins and orientations thus obtained to refine the low-defocus image using cross common lines (Simplex program); (iii) reconstructing an improved map from the low-defocus image which is used as a model for determining the origins and orientations for the high-defocus image in step (i). Using the low-defocus reconstruction as a model for directly refining the low-defocus data proved to be unsatisfactory. For the dodecahedron with fibre, the fibre density was not included in the model for orientation determination using the model-based programs, but it was included in the cross common lines refinement. For the final reconstruction in each case (Figure 2A and B), only particles from one negative were included and no correction for the CTF was made.

The reconstructions of the dodecahedra with and without fibre were made from micrographs with different defocus and hence different CTFs. Thus, in order better to compare the density maps, the average radial amplitude of the particle Fourier transforms for the reconstruction of dodecahedron without fibre were forced to that of the dodecahedron with fibre and the density map was recalculated to 25 Å resolution. The fibre density was not included in the comparison and the average radial density was slightly smoothed. This was not a complete CTF correction, just a minimal correction to bring the CTF of one reconstruction into line with another.

Isosurface representations of the reconstructed density were visualized using Explorer on an SGI.

Acknowledgements

We wish to thank S.Fuller for helpful advice and supplying his latest versions of the MRC icosahedral programs, J.-P.Eynard and F.Metoz for assistance in running the computers, and R.H.Wade for support. This is publication no. 418 of the Institut de Biologie Structurale Jean-Pierre Ebel.

References

Baker,T. and Cheng,R.H. (1996) A model-based approach for determining orientation of biological macromolecules imaged by cryoelectron microscopy. *J. Struct. Biol.*, **116**, 120–130.

Chroboczek,J., Ruigrok,R.W.H. and Cusak,S. (1995) Adenovirus fiber.In Doerfler,W. and Böhm,P. (eds), *Current Topics in Microbiology and Immunology. The Molecular Repertoire of Adenovirus I.* Vol. 199/I, Springer-Verlag, Berlin, pp. 164–200.

Crowther,R.A. (1971) Procedures for three-dimensional reconstruction of spherical viruses by Fourier synthesis from electron micrographs. *Phil. Trans. R. Soc. London Ser. B.*, **261**, 221–230.

Cuzange,A., Chroboczek,J. and Jacrot,B. (1994) The penton base of human adenovirus type 3 has the RGD motif. *Gene*, **146**, 257–259.

Devaux,C., Caillet-Boudin,M.-L., Jacrot,B. and Boulanger,P. (1987) Crystallization, enzymatic cleavage, and polarity of the adenovirus type 2 fiber. *Virology*, **161**, 121–128.

Fender,P., Ruigrok,R.W.H., Gout,E., Buffet,S. and Chroboczek,J. (1997) Adenovirus dodecahedron, a new vector for human gene transfer. *Nature Biotechnol.*, in press.

Fitzgerald,D.J.P., Padmanabhan,R., Pastan,I. and Wilingham,M.C. (1983) Adenovirus-induced release of epidermal growth factor and Pseudomonas toxin into the cytosol of KB cells during receptor-mediated endocytosis. *Cell*, **32**, 607–617.

Fuller,S.D., Butcher,S.J., Cheng,R.H. and Baker,T.S. (1996) Three-dimensional reconstruction of icosahedral particles. The uncommon line. *J. Struct. Biol.*, **116**, 48–55.

Furcinetti,P.S., van Oostrum,J. and Burnett,R.M. (1989) Adenovirus polypeptide IX revealed as capsid cement by difference images from electron microscopy and crystallography. *EMBO J.*, **8**, 3563–3570.

Green,N.M., Wrigley,N.G., Russell,W,C., Martin,S.R. and McLachlan,A. (1983) Evidence for a repeating cross-β sheet structure in the adenovirus fibre. *EMBO J.*, **2**, 1357–1365.

Henry,L., Xia,D., Wilke,M., Deisenhofer,J. and Gerard,R.D. (1994) Characterization of the knob domain of the adenovirus type 5 fiber protein expressed in *Escherichia coli*. *J. Virol.*, **68**, 5239–5246.

Hewat,E.A., Booth,T.F., Loudon,P.T. and Roy,P. (1992a) Three dimensional reconstruction of baculovirus expressed bluetongue virus core-like particles by cryo-electron microscopy. *Virology*, **189**, 10–20.

Hewat,E.A., Booth,T.F. and Roy,P. (1992b) Structure of bluetongue virus particles by cryoelectron microscopy. *J. Struct. Biol.*, **109**, 61–69.

Horwitz,M.S. (1990) Adenoviridae and their replication. In Field,B.N. and Knipe,D.M. (eds), *Virology.* Raven Press, New York, pp. 1680–1721.

Kidd,A.H., Chroboczek,J., Cusack,S. and Ruigrok,R.W.H. (1993) Adenovirus type 40 virions contain two distinct fibres. *Virology*, **192**, 73–84.

Laver,W.G., Wrigley,N.G. and Pereira,H.G. (1969) Removal of pentons from particles of adenovirus type 2. *Virology*, **39**, 599–605.

Louis,N., Fender,P., Barge,A., Kitts,P. and Chroboczek,J. (1994) Cell-binding domain of adenovirus serotype 2 fiber. *J. Virol.*, **68**, 4104–4106.

Mathias,P., Wickham,T., Moore,M. and Nemerow,G. (1994) Multiple adenovirus serotypes use αv integrins for infection, *J. Virol.*, **68**, 6811–6814.

Nermut,M.V. (1984) The architecture of adenoviruses. In Ginsberg,H.S. (ed.), *The Adenoviruses.* Plenum Press, New York, pp. 5–34.

Norrby,E. (1964) The relationship between the soluble antigens and the virion of adenovirus type 3. I. Morphological characteristics. *Virology*, **1**, 236–248.

Philipson,L., Lonberg-Holm,K. and Petterson,U. (1968) Virus-receptor interaction in an adenovirus system. *J. Virol.*, **2**, 1064–1075.

Roberts,M.M., White,J.L., Grütter,M.G. and Burnett,R.M. (1986) Three dimensional structure of the adenovirus major coat protein hexon. *Science*, **232**, 1148–1151.

Ruigrok,R.W.H., Barge,A., Albizes-Rizo,C. and Dayan,S. (1990) Structure of adenovirus fibre. II. Morphology of single fibers. *J. Mol. Biol.*, **215**, 589–596.

Signäs,C., Akusjärvi,G. and Pettersson,U. (1985) Adenovirus 3 fibre polypeptide gene: implications for the structure of the fibre protein. *J. Virol.*, **53**, 672–678.

Stewart,P.L., Burnett,R.M., Cyrklaff,M. and Fuller,S.D. (1991) Image reconstruction reveals the complex molecular organization of adenovirus. *Cell*, **67**, 145–154.

Stewart,P.L., Fuller,S.D. and Burnett,R. (1993) Difference imaging of adenovirus: bridging the resolution gap between X-ray crystallography and electron microscopy. *EMBO J.*, **12**, 2589–2599.

Stouten,P.F.W., Sander,C., Ruigrok,R.W.H. and Cusack,S. (1992) New triple-helical model for the shaft of Adenovirus fibre. *J. Mol. Biol.*, **226**, 1073–1084.

van Oostrum,J., Smith,P.R., Mohraz,M. and Burnett,R.M. (1987) The structure of the adenovirus capsid. III. Hexon packing determined from electron micrographs of capsid fragments. *J. Mol. Biol.*, **198**, 73–89.

Verdaguer,N., Mateu,M.G., Andreu,D., Giralt,E., Domingo,E. and Fita,I. (1995) Structure of the major antigenic loop of foot-and-mouth disease virus complexed with a neutralizing antibody: direct involment of the Arg-Gly-Asp motif in the interaction. *EMBO J.*, **14**, 1690–1696.

Wickham,T., Mathias,P., Cheresh,D.A. and Nemerow,G.R. (1993) Integrins $\alpha_v\beta_3$ and $\alpha_v\beta_5$ promote adenovirus internalisation but not virus attachement. *Cell*, **73**, 309–319.

Xia,D., Henry,L.J., Gerard,R.D. and Deisenhofer,J. (1994) Crystal structure of the receptor-binding domain of adenovirus type 5 fibre protein at 1.7 Å resolution. *Structure*, **2**, 1259–1270.

Yang,Y., Li,Q., Ertl,H.C.J. and Wilson,J.M. (1995) Cellular and humoral immune response to viral antigens create barriers to lung-directed gene therapy with recombinanat adenoviruses. *J. Virol.*, **69**, 2004–2015.

Yoshimura,K., Rosenfeld,M.A., Seth,P. and Crystal,R.G. (1993) Adenovirus-mediated augmentation of cell transfection with unmodified plasmid vectors. *J. Biol. Chem.*, **268**, 2300–2303.

Received on July 12, 1996; revised on August 27, 1996